

Improvise, Adapt, Overcome: An On-The-Fly Multifidelity Algorithm for Efficient Machine Learning

Vivin Vinod^{1*} and Peter Zaspel¹

¹School of Mathematics and Natural Sciences, University of Wuppertal, Germany.

*Corresponding author(s). E-mail(s): vinod@uni-wuppertal.de

Abstract

Machine learning has accelerated quantum chemistry but is hindered by the prohibitive cost of generating high fidelity training data. Multifidelity machine learning (MFML) mitigates this overhead by systematically combining abundant low fidelity data with sparse high fidelity data. In spite of its success, standard MFML schemes rely on pre-defined scaling factors to determine sparse data ratio across fidelities, often generating redundant multifidelity data resulting in a loss of efficiency. Here, we introduce an adaptive on-the-fly multifidelity framework for machine learning that autonomously determines training dataset composition. By dynamically querying training samples at each fidelity, the algorithm saturates model accuracy at lower fidelities before moving up to more expensive reference calculations. We benchmark the novel adaptive-MFML across diverse chemical properties including the computational chemistry gold standard coupled cluster energies, and the more chemically challenging excitation energies. In our numerical experiments we show that our adaptive algorithm reduces data generation costs by up to a factor of 30 compared to single fidelity methods and improves upon standard MFML by up to a factor of 5. The mitigation of data redundancy establishes a high-accuracy low-cost pathway for sustainable cost-aware machine learning in quantum chemistry.

1 Introduction

In computational simulations, increasing the cost-budget typically yields higher accuracy, introducing the concept of *fidelities* relative to a ground truth [1, 2]. The

cost-accuracy tradeoff is central in multifidelity methods where the aim is to achieve high-accuracy low-cost models by strategically combining outputs across fidelities. These methods often utilize data-driven surrogates, such as machine learning (ML) models, to *comprehensively correct* a low fidelity (computationally cheap) model to match the accuracy of the higher fidelity model at a much lower cost than running the higher fidelity model. Multifidelity methods have seen a wide range of applications ranging from geological sciences to fluid simulations [3].

The use of ML has significantly accelerated research in quantum chemistry (QC), replacing costly calculations with accurate predictions [4, 5]. However, these surrogate models require substantial training data and are usually restricted to the fidelity of the training data. This caveat has been of some discussion only in the recent past, with increasing notice being paid to this computational bottleneck. High accuracy reference data, such as the gold standard of Coupled Cluster with Singles, Doubles, and Perturbative Triples (CCSD(T)), scales prohibitively with system size as $\mathcal{O}(N^7)$ [6] severely limiting the ML-QC workflow for high fidelity QC properties.

Multifidelity machine learning (MFML) has emerged as a prominent solution to the training data cost bottleneck. Following the *ansatz* of standard multifidelity methods [1, 2], the comprehensive correction of low fidelity ML models towards high fidelity QC predictions has been used successfully to predict properties ranging from ground state energies to excitation energies and bandgaps of solids showing significant reduction in the time-cost of the ML-QC pipeline [7–12]. With increasing interest in sustainable chemical discovery and reducing computation footprint of ML in QC [13], MFML methods have increasingly become popular not only for their prediction accuracy but also for their ability to reduce the computation cost incurred [10, 14, 15]. While the MFML methods are well established for small, isolated molecules [14, 16], they also show great promise for scalability in extended molecular systems. Recent applications highlight this capability, ranging from simulating exciton energy transfer in a collection of 85-atom porphyrins on a clay surface for synthetic light-harvesting [17] to over 3.5 million point predictions of high fidelity excitation energies in a light harvesting complex of photosynthetic bacteria [18].

In spite of their success, standard MFML methods address data sparsity with increasing fidelity by relying on a fixed scaling factor to determine the ratio of training samples between two fidelities. Conventionally, the scaling factor is set to 2 [9, 10] derived from legacy of sparse grid combination techniques [19]. Other fixed values of the scaling factor have been explored indicating that larger values improve the cost-benefit effectiveness of the MFML models [16, 17]. An alternate approach for the use of multifidelity methods in ML-QC introduced an *ad-hoc* heuristic to dictate training data set sizes across fidelities omitting the fixed scaling factor [14]. The scheme, hierarchical ML, uses several Δ -ML models [7] and assumes a constant ratio of predictions between two Δ -ML models for subsequent fidelities remains approximately constant. This scheme was shown to be effective in reducing training data costs for a specific isolated small molecule by a factor of 100. In such a setup, a noted constraint is that the constant ratio assumption breaks down for small training set sizes and requires a *post-hoc* optimization. Further, since the error is estimated, an *a-posteriori* calibration of the final trained model could be required. Ultimately, both fixed scaling factor MFML

and *ad-hoc* estimated training dataset sizes fail to dynamically capture the true cost-benefit contribution of each fidelity during training the MFML model. Inevitably, this leads to an increased risk of redundancy of costly training data generation requiring manual *post-hoc* intervention.

With cost-aware ML gaining traction in QC, there is a pressing need to develop robust adaptive schemes for the dynamic selection of optimal number of training samples per fidelity. Such an algorithm would not only minimize expensive training data generation but also relies on an on-the-fly computation of reference QC properties. Unlike conventional MFML approaches that require *a-priori* datasets across all fidelities, a truly adaptive sampling scheme queries QC reference calculations strictly on a need-to-know basis eliminating redundancy in the ML-QC pipeline by generating only the data necessary to improve the model.

This work introduces a novel adaptive-MFML scheme that performs on-the-fly sampling of training data at each fidelity to minimize the empirical error of the resulting MFML model. Recursively adding training samples at each fidelity, the algorithm ensures the error reduction meets a user-defined threshold. We demonstrate in the following section that this new adaptive algorithm reduces the computation cost of ML-QC methods by several orders of magnitude compared to single fidelity methods, and improves on basic MFML baselines by a factor of 5 in some cases. The algorithm is shown to be robust and reduce redundancy. The broad applicability of the proposed adaptive-MFML framework across diverse QC properties is demonstrated by predicting properties ranging from *ab initio* potential energy surfaces (PES) to more complex excitation energies.

2 Results

The conceptual workflow of the adaptive sampling framework for MFML models is depicted in Fig. 1. The multifidelity training dataset is initialized using a few randomly sampled geometries with corresponding QC properties computed at varying fidelities. Across all experiments presented herein, we define four discrete fidelities, $f \in \{1, 2, 3, 4\}$, with the initial dataset size $N_{\text{train}} = [32, 16, 8, 4]$, that is, 32 training samples at fidelity 1, 16 at fidelity 2 and so on. This reflects a small basic MFML architecture. The algorithm itself operates in a nested loop structure. In the local loop (hereon also referred to as an epoch), the algorithm dynamically adds training data starting with the lowest fidelity. During each epoch, an MFML model of the corresponding training data set composition is trained and evaluated against a small validation set of high-fidelity reference computations to keep track of the prediction error computed as the mean absolute error (MAE; see section 4.3). To avoid pre-asymptotic artifacts that arise due to very small dataset sizes, the improvement of the MFML model is assessed over a moving average of the MAE. If the improvement falls below a predefined *local tolerance*, the algorithm advances to the next fidelity to carry out on-the-fly querying of training data. The algorithm allows one to set individual local tolerance values per fidelity which can arise from domain expertise on what improvement is expected for a fidelity. For instance, it is reasonable to claim that

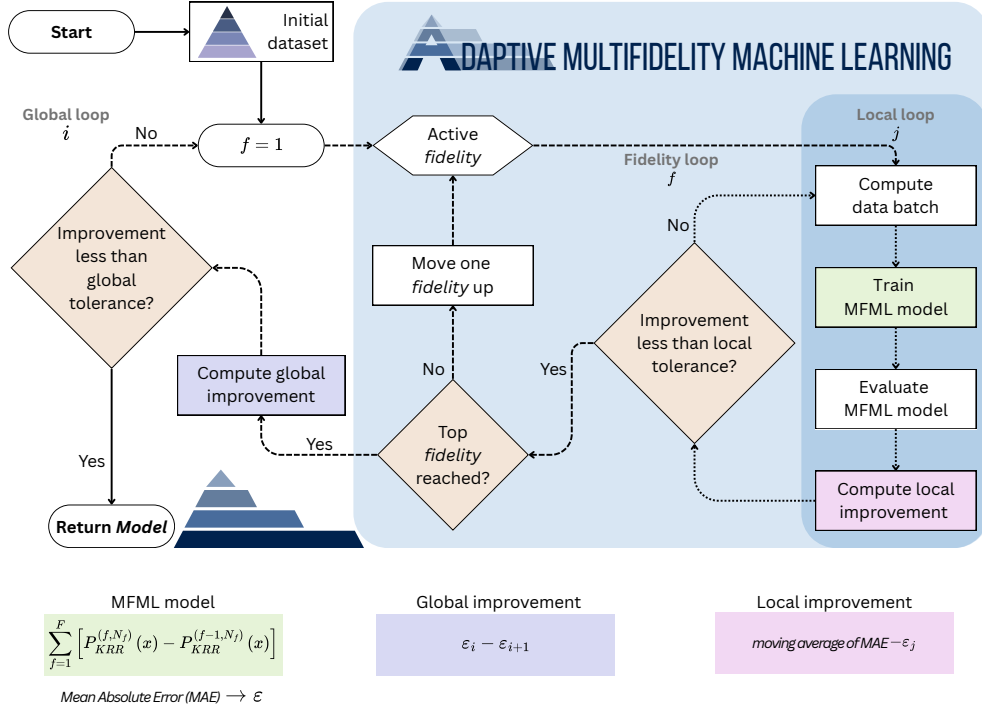


Fig. 1 The conceptual workflow of adaptively selecting training samples at each fidelity. The local loop performs on-the-fly computations of QC properties for a given fidelity. Tolerance checks at each fidelity and at the global level, that is once all fidelities have been accessed once, ensure prevention of redundant training data generation.

the addition of a geometry with high fidelity reference computed should give better prediction accuracy compared to the same geometry with a low fidelity reference.

This step-wise progression of fidelities is carried out until the highest fidelity is reached, completing one *global loop*. On completing a global loop, the algorithm checks the overall error reduction across the full pass from lowest to highest fidelity. If the error has improved compared to the previous pass, the sequence restarts at the lowest fidelity. If the improvement is below a set threshold of *global tolerance*, the algorithm terminates returning the adaptively sampled multifidelity training dataset and the final trained model. This form of aggressive pruning of redundant reference computation queries and growing a dataset strictly on a need-to-know basis allows the adaptive framework to avoid *a-priori* generation of expensive data directly addressing the cost-budget bottleneck in the ML-QC pipeline.

In order to establish the efficacy of the novel adaptive sampling method, we MAE using holdout test sets that are unseen in both training and algorithmic looping. This ensures that errors reflect true generalization. A comparison of the validation set error (used to carry out sampling in the adaptive algorithm) and the holdout test set error are presented in the supplementary information SF3 to reason that the validation set

error does match the test set error indicating that the algorithm is indeed robust for generalization. The core ML architecture used in this work is Kernel Ridge Regression (KRR) motivated by its proven robustness in multifidelity QC applications [9, 14, 16].

For each experiment, the total geometries are partitioned into a train:validation:test split of 85:5:10. We simulate the on-the-fly nature of the adaptive-MFML algorithm by querying the pre-computed QC reference values from the datasets only when requested in the epoch. The adaptive-MFML method is benchmarked against two baselines: a single fidelity KRR model trained only on highest fidelity data, and a standard MFML model where data sparsity is dictated by the conventional fixed scaling factor of 2 (that is, $N_{\text{train}}^{f-1} = 2 \cdot N_{\text{train}}^f$). We carry out a 10-fold cross validation to assess the holdout test set prediction error for all three methods. For MFML methods, cross validation is carried out with adherence to a nested data structure (see section 4.1) requirement outlined in Ref. [20]. We analyze the MAE of each model as a function of the cumulative time-cost incurred in training data generation (see section 4.3). For single fidelity models, the cost is the product of the highest fidelity per sample cost and the training set size. For the MFML models, the cost is the sum of costs across all queried fidelities. An assessment of these time-cost learning curves provides a direct measure of data efficiency making it a critical metric in understanding the computational footprint of cost-aware ML models in QC.

2.1 Coupled Cluster Potential Energy Surfaces

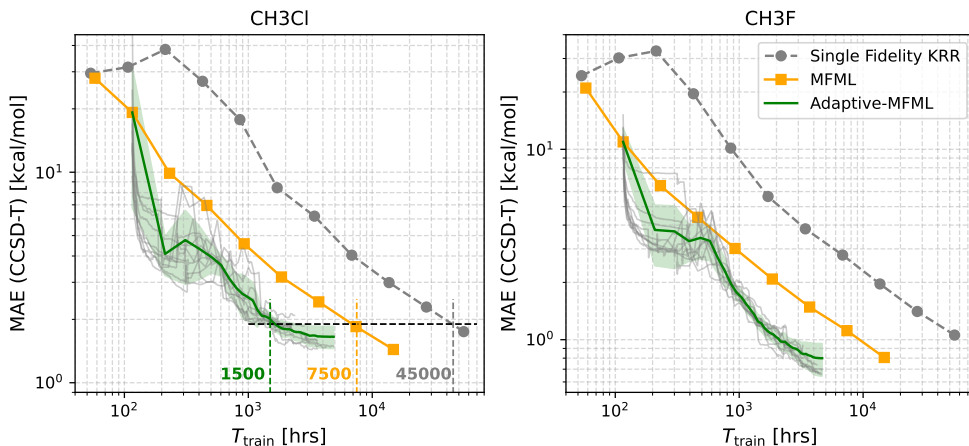


Fig. 2 Time-cost of training data versus MAE for prediction of *ab initio* potential energy surfaces at the CCSD(T) level for CH_3Cl and CH_3F of the VIB5 dataset[21]. The adaptive-MFML model achieves the target MAE at a significantly lower computational cost than both standard MFML and single fidelity KRR.

The VIB5 dataset provides high accuracy *ab initio* potential energy surfaces (PES) for CH_3Cl and CH_3F molecules [21]. For each molecule, we consider four fidelity levels,

listed in increasing order of computation cost: HF/cc-pVTZ, HF/cc-pVQZ, MP2/cc-pVTZ, and CCSD(T)/cc-pVQZ (see Supplementary Information S3 for comprehensive details). Fig. 2 presents the MAE as a function of training data generation time-cost for three distinct methods: single fidelity KRR, standard MFML, and adaptive-MFML. For the adaptive-MFML, we report the averaged learning curve as well as the independent-run trajectories.

Consider the curves for CH₃Cl on the left side of Fig. 2. The horizontal and vertical dashed lines indicate the time-cost required to reach a target MAE of ~ 2 kcal/mol. To achieve this accuracy, single fidelity KRR demands $T_{\text{train}} = \sim 45,000$ hrs of compute budget whereas the standard MFML model requires $\sim 7,500$ hrs. Remarkably, the adaptive-MFML reaches this target error with just ~ 1500 hrs. This translates to a 30-fold improvement over single fidelity KRR and a 5-fold reduction of time cost in comparison to the standard MFML approach. A similar efficiency gain is observed for CH₃F, indicating robust performance of the algorithm. For both the molecules, across independent instantiations, adaptive-MFML exhibits a consistent trend. Each epoch systematically reduces the MAE, and the individual runs converge to the averaged curve.

2.2 Ground State and Vertical Excitation Energies

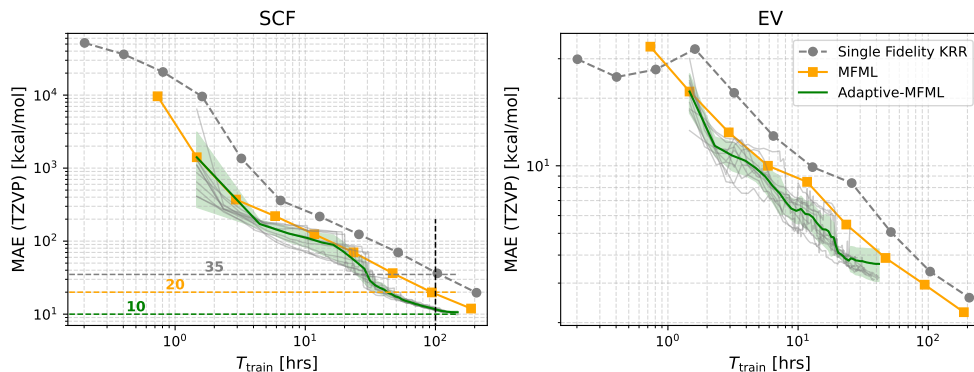


Fig. 3 Model error (MAE) as a function of training data generation time-cost for single fidelity KRR, basic MFML, and adaptive-MFML on the QeMFi dataset [22, 23]. For a fixed time-cost budget, the adaptive-MFML is seen to be the most beneficial with the lowest achieved MAE for both ground state (SCF) and vertical excitation energies (EV).

The QeMFi dataset [22, 23] provides a more complex chemical challenge than the VIB5 dataset consisting of nine chemically diverse molecules with geometries sampled from Wigner distributions [24]. For each of the 135,000 geometries, electronic properties, including ground state self-consistent field (SCF) energies and vertical excitation (EV) energies, are computed using the TD-DFT formalism with the CAM-B3LYP functional. The multifidelity hierarchy is defined by increasing basis set sizes: 3-21G, 6-31G, def2-SVP, def2-TZVP (see Supplementary Information S3 for details).

We evaluate the novel adaptive-MFML method on both the SCF energies and the more challenging vertical excitation energies. Fig. 3 presents the time-cost versus MAE curves for these properties. Analyzing the SCF energy predictions presents an alternative perspective on model performance, that is, evaluating accuracy under a strict computational budget as opposed to considering a target MAE (as studied in the case for VIB5). Given a fixed budget of, say, 100 hours, the single-fidelity model KRR results in an MAE of ~ 35 kcal/mol, and the standard MFML model reduces this to about 20 kcal/mol. In contrast the adaptive-MFML model achieves an MAE of ~ 10 kcal/mol representing a little over 3-fold improvement over single fidelity KRR, and a 2-fold improvement in accuracy over basic MFML.

Considering the vertical excitation energies on the right-hand side of Fig. 3, limiting the time-cost budget to about 20 hours results in an MAE of ~ 9 kcal/mol for the single fidelity KRR model and a ~ 6 kcal/mol for the basic MFML model. The adaptive-MFML model reduces this error to ~ 4 kcal/mol. While the relative performance gain of using the adaptive-MFML algorithm are markedly smaller here than those observed for SCF energies, it is to be noted that this is due to the inherent complexity of the excitation state energy landscape which are known to be difficult for ML models to capture well [25, 26]. Despite this universal challenge across ML in QC, the adaptive-MFML algorithm outperforms both the single fidelity KRR and basic MFML baselines.

2.3 Coupled Cluster Energies of ANI-1ccx

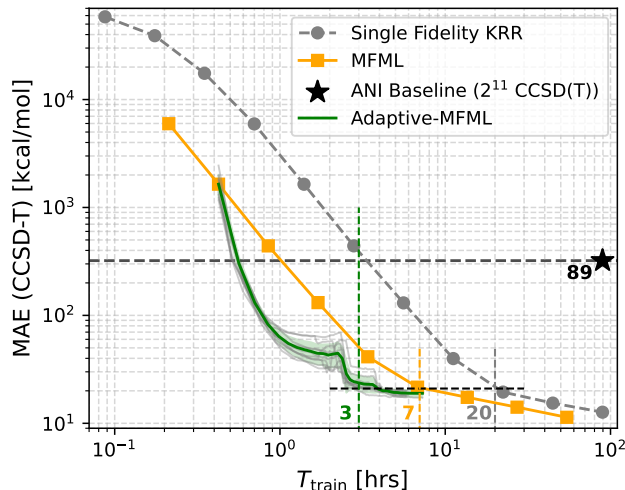


Fig. 4 Training data generation time-cost versus MAE for the ANI-1ccx dataset collection of molecules [27]. Kernel-based ML architectures achieve lower errors than the baseline ANI model trained on 2^{11} CCSD(T) samples. Furthermore, the novel adaptive-MFML method reaches a target error at the lowest overall time-cost.

Coupled cluster (CC) methods are widely regarded as the golden standard in QC. However, computing high fidelity properties at CC becomes prohibitive for molecules with more than a dozen atoms [28]. The ANI-1ccx dataset consists of several molecules of varying sizes with the fidelities HF/ccpVDZ, DFT- ω b97x/ccpVDZ, DFT- ω b97x/ccpVTZ, and the CCSD(T) [27] (see Supplementary Information S3 for data pre-processing and S4 for time-cost computation protocols). We contrast the performance of the single-fidelity KRR, basic MFML, and adaptive-MFML models for this hierarchy. In order to additionally establish a neural network baseline, we trained a single fidelity ANI model [29] using 2^{11} CCSD(T) training samples (see Supplementary Information S7 for training details).

Fig. 4 reports the learning curves for predicting molecular energies at the CCSD(T) fidelity. The baseline ANI model requires a computational budget of ~ 89 hours to yield a prediction error of ~ 320 kcal/mol. In stark contrast, even the single fidelity KRR model for the exact same time-cost achieves a significantly lower MAE of ~ 10 kcal/mol. The efficiency of the adaptive-MFML algorithm becomes evident on considering a target accuracy, say ~ 10 kcal/mol, as indicated by the lower horizontal dashed line. The single fidelity KRR model requires a time-cost budget of ~ 20 hours, the basic MFML model requires ~ 7 hours, and the adaptive-MFML model only needs ~ 3 hours. This represents an 8-fold improvement over single fidelity KRR and a little over a 2-fold improvement over the basic MFML approach.

For larger cost budgets, the learning curves for all three models begin to plateau out and saturate. That is, additional training data does not yield as strong an improvement in the models’ accuracy indicating an inherent structural complexity within the data. Crucially, since this saturation is observed for single fidelity KRR and the multifidelity models, it is not an artifact of the MFML or adaptive scheme itself but rather an intrinsic property of the underlying chemical space being learned.

To further analyze the adaptive-MFML model for the ANI-1ccx dataset, Fig. 5(a) presents the distribution of differences between predictions and reference CCSD(T) energies (that is $y^F - P_{\text{adaptive-MFML}}$). We select the adaptive-MFML model trained under a ~ 3 hour computational budget, which corresponds to the multifidelity training dataset composition of [768, 112, 28, 12]. The differences are centered around 0 kcal/mol indicating strong agreement between prediction and reference in most cases. For molecules with number of atoms ranging between 8-25, the error bars extend to about 40 kcal/mol on either side of 0 kcal/mol. While this might seem like a large fluctuation, it is worth noting that the energies themselves range between -400,000 kcal/mol and 200,000 kcal/mol as seen in Fig. SF5 of the supplementary information. Indeed Fig. SF5 presents that the predictions and references from this adaptive-MFML model lies near-perfectly on the identity line indicating very good agreement. A detailed assessment on this can be found in section S8 of the supplementary information.

Fig. 5(b) presents MAEs binned by the number of atoms in the molecules of the ANI-1ccx dataset. The highest recorded MAE occurs in the 43-atom bin. However, as shown in Fig. 5(a), this represents a single outlier molecule in the test set and should not therefore be representative of the general model. Examining bins of more representative sampling, such as molecules with 14 atoms, result in an MAE of 15.67

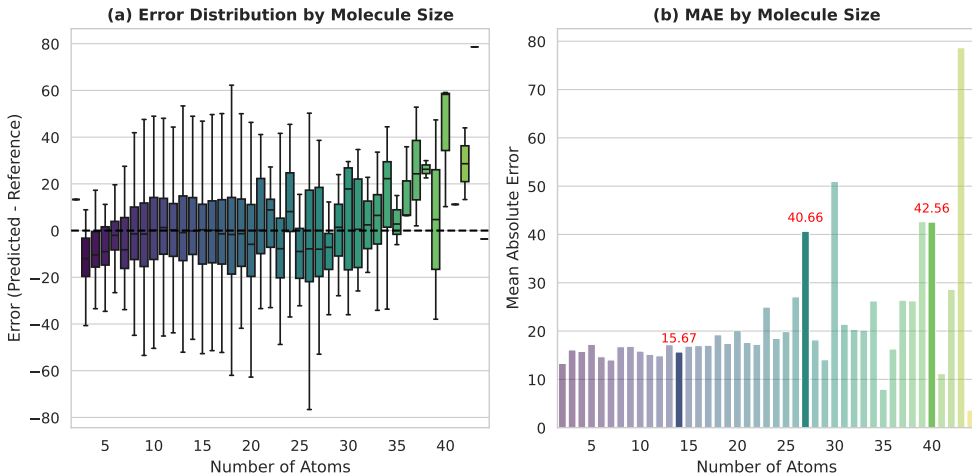


Fig. 5 (a) Distribution of prediction error for the adaptive-MFML model (trained for a ~ 3 hrs time-cost budget), categorized by molecule size in the ANI-1ccx dataset. (b) MAE of the same adaptive-MFML model, binned by the number of atoms per molecule.

kcal/mol. Meanwhile, an MAE of ~ 40 kcal/mol is seen for molecules with 27 and 40 atoms each. Overall, the MAE distribution on the basis of the number of atoms in the molecule have a low value for most of the bins underscoring the predictive accuracy of the adaptive-MFML model across varying molecular size.

To substantiate the broad statistical analysis above, we examine predictions for a few randomly selected molecules from the test set of the ANI-1ccx dataset. We compare three models: the baseline ANI model trained on single fidelity CCSD(T) data (time-cost of ~ 89 hours), single fidelity KRR model trained on 2^6 CCSD(T) data points (time-cost ~ 3 hours), and the adaptive-MFML model with training dataset composition [768, 112, 28, 12] (time-cost ~ 3 hours). The single fidelity KRR and adaptive-MFML models are trained with the same time-cost budget. Fig. 6 reports the absolute value of prediction error, $|y^F - P_{ML}|$, for a random selection of molecules from the test set. The baseline model exhibits the highest discrepancy between predicted and reference energies. For all the molecules, the adaptive-MFML model consistently yields the lowest error. This confirms that the adaptive-MFML algorithm not only reduces training data costs to reach a target representative error, but that it also faithfully reproduces the high-fidelity reference energies for molecules of diverse sizes.

3 Discussion

The generation of high-fidelity training data remains a prohibitive hurdle for the successful and sustainable use of ML in QC. While standard MFML significantly reduces the computational cost, reliance on rigid heuristics for training dataset composition limits the maximum achievable efficiency in these methods. The adaptive algorithm for MFML that is developed in this work addresses this directly by dynamically growing

Prediction error in kcal/mol for molecules of ANI-1ccx dataset for the ANI, Single Fidelity KRR, and Adaptive-MFML (this work) models. The single fidelity and MFML models are built with training samples that cost the same (see main text).

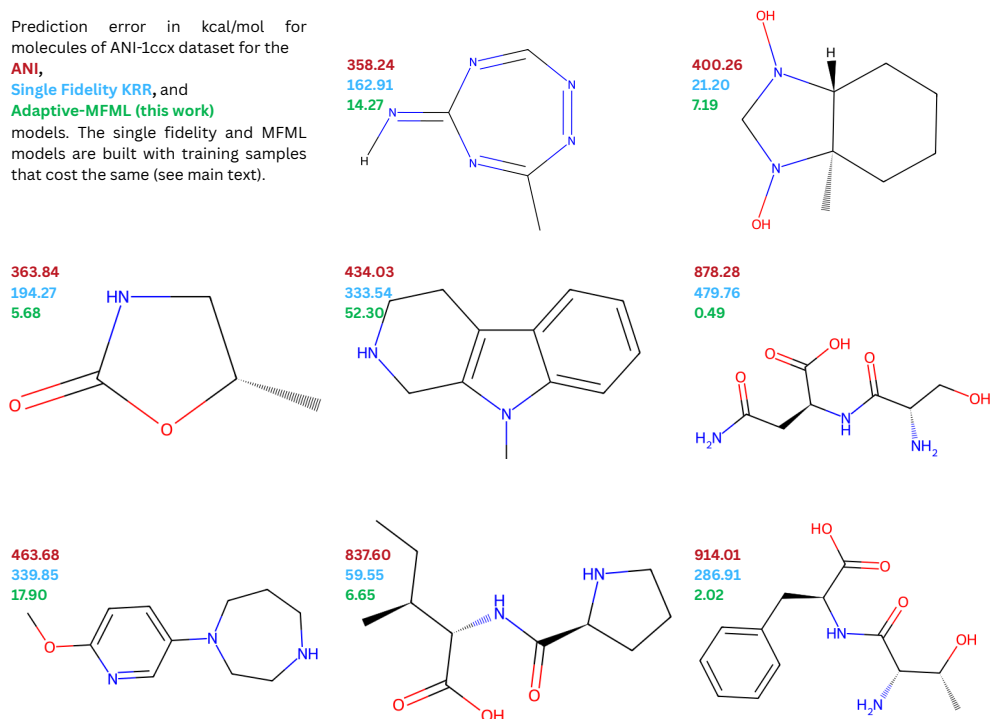


Fig. 6 Difference between predicted and reference CCSD(T) energies for selected molecules across three ML models: the baseline ANI model trained on 2^{11} CCSD(T) samples (denoted by the starred dotted line in Fig. 4; ~ 89 hours of time-cost), a single fidelity KRR model trained on 2^6 CCSD(T) samples (~ 3 hours of time-cost), and the adaptive-MFML model (~ 3 hours of time-cost). The adaptive-MFML model consistently achieves the lowest MAE, confirming that the efficiency gain translates into robust individual molecular predictions.

the training datasets on-the-fly ensuring further streamlining of cost budgets in such models. Our numerical experiments validate the efficacy of this algorithm for diverse QC properties ranging from gold standard CCSD(T) energies to hard-to-learn excitation energies. While fixed scaling factor MFML assumes a uniform rate of information gain across all fidelities, the adaptive method inherently measures the marginal information gain of each batch of training samples added. If a lower fidelity does capture the underlying physical characteristic of the QC property, the algorithm ‘recognizes’ this and limits the querying of high-fidelity reference computations. A variant of the herein developed adaptive algorithm is evaluated separately in Supplementary Information S9 to provide an exhaustive analysis of this approach for MFML.

While the adaptive-MFML framework demonstrates high efficiency and accuracy in the results above, several open areas of research can be identified. Formulating the dataset size at each fidelity as hyper-parameters to be optimized via a differentiable objective function is one such promising direction. Recent advances in active learning

to guide geometry sampling for the chemical configuration space using low fidelity reference data promise improvement in prediction accuracy by an order of magnitude [30]. The modular nature of the adaptive algorithm enables seamless integration with such active learning schemes to further improve the cost efficiency of multifidelity methods. The adaptive-MFML method is certainly not without limitations. One immediate observation is that dataset generation for standard MFML allows for parallelization of training data generation across fidelities whereas in the adaptive-MFML algorithm, since reference calculations are on demand, it introduces a sequential limitation on the data generation. However, the efficacy of the method ought to make up for this limitation. One potential solution to this serialization is the use of pre-trained global machine learning interatomic potentials (MLIPs) [31, 32] to further reduce the cost of making actual computations. Such an approach would come with its own challenge of recursive training of ML models on their own outputs and is an interesting area of research.

Overall the adaptive-MFML method represents a substantial leap forward in cost-aware sustainable QC. it offers a noticeable improvement not only over single fidelity methods but also over conventional MFML paradigms. By dynamically mitigating data redundancy, it provides a highly efficient solution across diverse QC properties and complex molecular spaces. We have made the associated source code fully open-access and well documented, ensuring this adaptive framework is readily deployable for the broader computational community.

4 Methods

Details regarding Kernel Ridge Regression (KRR) architecture, dataset composition, and molecular descriptor generation are provided Supplementary Information sections S1–S3.

4.1 Multifidelity Machine Learning

Let an ordered set of fidelities $f = \{1, 2, \dots, F\}$ be given such that the accuracy of the evaluation of the computation (the oracle), $g^f(\mathbf{x}) = y^f$ is greater than the accuracy of $g^{f-1}(\mathbf{x}) = y^{f-1}$. Thus, $\mathcal{T}^f := \left\{ (\mathbf{x}_i, y_i^f) \right\}_{i=1}^{N_f}$ represents the training set at fidelity f . A recursive comprehensive correction of fidelities formulated for unseen input features \mathbf{x}_q as

$$P^f(\mathbf{x}_q) := \rho_{f-1}(\mathbf{x}_q)P^{f-1}(\mathbf{x}_q) + \delta_f(\mathbf{x}_q), \quad (1)$$

where P^f is the output from a surrogate model for fidelity f , ρ is the multiplicative corrective term, and δ is the additive correction term [2]. Multifidelity machine learning uses this concept and generalizes it to train sub-models at different fidelities [9, 20]. Each sub-model is identified by the fidelity f and the number of training samples N . That is, a composite index $\mathbf{s} := (f, N)$ is used. The number of training samples halves at each successive fidelity, that is, $N_{f-1} = 2 \cdot N_f$. Since data sparsity increases with increase in fidelity of data, MFML requires a nested training data structure [33]. Define

$\mathcal{X}^f := \{\mathbf{x}_i | (\mathbf{x}_i, y_i^f) \in \mathcal{T}^f\}$. The nestedness of multifidelity data is then expressed as:

$$\mathcal{X}^F \subseteq \mathcal{X}^{F-1} \subseteq \dots \subseteq \mathcal{X}^1 .$$

For a query descriptor \mathbf{x}_q the final high fidelity prediction is the linear combination of sub-model predictions:

$$P_{\text{MFML}}(\mathbf{x}_q) := \sum_{\mathbf{s} \in \mathcal{S}} \beta_{\mathbf{s}} P_{\text{ML}}^{\mathbf{s}}(\mathbf{x}_q) , \quad (2)$$

where \mathcal{S} is the set of all sub-models selected to be part of the MFML structure [20]. For a given baseline fidelity (f_b), that is the lowest fidelity to be used in the MFML model, target fidelity (F), and number of training samples at the target fidelity (N_F), one can write:

$$\begin{aligned} \mathcal{S} := \{ & (f, N_F) \mid f \in \{f_b, \dots, F\}, \\ & N_F \in \{N_F, \dots, 2^{F-f_b} \cdot N_F\}, \\ & F + N_F - 1 \leq f + N_F \leq F + N_F \} , \end{aligned}$$

The coefficients $\beta_{\mathbf{s}}$ are assigned unitary signed values (± 1). In this work, we utilize a KRR architecture for the sub-models $P_{\text{ML}}^{\mathbf{s}}$. However, it must be noted that the MFML scheme is architecture-agnostic and can be implemented for alternate architectures such as neural networks [8].

As an example, consider a three fidelity hierarchy, that is, $f = \{1, 2, 3\}$ with $N_F = 4$. Then, the prediction from the MFML model using the KRR architecture for the sub-models is given as

$$\begin{aligned} P_{\text{MFML}}(\mathbf{x}_q) := & P_{\text{KRR}}^{(f=3,4)}(\mathbf{x}_q) - P_{\text{KRR}}^{(f=2,4)}(\mathbf{x}_q) \\ & + P_{\text{KRR}}^{(f=2,8)}(\mathbf{x}_q) - P_{\text{KRR}}^{(f=1,8)} \\ & + P_{\text{KRR}}^{(f=1,16)}(\mathbf{x}_q) . \end{aligned}$$

This expansion reveals that the prediction of an MFML model can be seen as a telescopic sum across fidelities:

$$P_{\text{MFML}}(\mathbf{x}_q) := \sum_{f=1}^F \left[P_{\text{KRR}}^{(f, N_f)}(\mathbf{x}_q) - P_{\text{KRR}}^{(f-1, N_f)}(\mathbf{x}_q) \right] , \quad (3)$$

where we define $P_{\text{KRR}}^{(0, N)}(\mathbf{x}_q) \equiv 0$ explicitly.

4.2 Adaptive Multifidelity Sampling

The MFML scheme described above has been successfully used to reduce training data costs for various QC properties such as excitation energies [10, 20] and atomization

Algorithm 1 Adaptive Multifidelity Sampling algorithm for an ordered hierarchy of fidelities $f \in \{1, 2, \dots, F\}$.

Require: initial training set sizes $\mathbf{N}_{\text{train}} := [N_1, N_2, \dots, N_F]$, batch sizes $\mathbf{m}_{\text{batch}} := [m_1, m_2, \dots, m_F]$, local tolerances $\boldsymbol{\tau} := [\tau_1, \tau_2, \dots, \tau_F]$, global tolerance τ_{global} , validation dataset \mathcal{V}^F

Ensure: QC calculator $g_{\text{QC}}^f, \forall f \in \{1, \dots, F\}$

- 1: $\mathcal{T}^f \leftarrow \left\{ (x_i, g_{\text{QC}}^f(x_i)) \right\}_{i=1}^{N_f}, \forall f \in \{1, \dots, F\}$
- 2: $\mathcal{T}_{\text{MFML}} \leftarrow [\mathcal{T}^1, \dots, \mathcal{T}^F]$ ▷ Initial multifidelity dataset
- 3: $\Delta \leftarrow \text{MAE}(\mathcal{T}_{\text{MFML}}, \mathcal{V}^F)$ ▷ Initialize local improvement
- 4: $\Delta_{\text{global}} \leftarrow \Delta$ ▷ Initialize global improvement
- 5: **while** $\Delta_{\text{global}} > \tau_{\text{global}}$ **do** ▷ Repeat the sampling scheme
- 6: **for** $f = 1$ **to** F **do** ▷ Step up through each fidelity
- 7: **while** $\Delta > \tau[f]$ **do** ▷ Sample at fidelity f
- 8: **if** $f > 1$ and $2 \times (\mathbf{N}_{\text{train}}[f] + \mathbf{m}_{\text{batch}}[f]) \geq \mathbf{N}_{\text{train}}[f - 1]$ **then**
- 9: **break** ▷ Maintain hierarchical size constraint
- 10: **end if**
- 11: $\mathcal{T}_{\text{batch}}^f \leftarrow \left\{ (x_i, g_{\text{QC}}^f(x_i)) \right\}_{i=1}^{\mathbf{m}_{\text{batch}}[f]}$ ▷ **On-the-fly computations**
- 12: $\mathcal{T}^f \leftarrow \mathcal{T}^f \cup \mathcal{T}_{\text{batch}}^f$ ▷ Add samples at current fidelity
- 13: $\mathcal{T}_{\text{MFML}} \leftarrow [\mathcal{T}^1, \dots, \mathcal{T}^f, \dots, \mathcal{T}^F]$ ▷ Update multifidelity training data
- 14: $E \leftarrow \text{MAE}(\mathcal{T}_{\text{MFML}}, \mathcal{V}^F)$
- 15: $\Delta \leftarrow \text{Local_Improvement}(E)$ ▷ e.g., change in moving average
- 16: **end while**
- 17: **end for**
- 18: $\Delta_{\text{global}} \leftarrow \text{Global_Improvement}(E)$
- 19: **end while**
- 20: **return** $\mathbf{N}_{\text{train}}, \mathcal{T}^f, \forall f \in \{1, 2, \dots, F\}$

energies [9]. However, in the standard MFML model, the number of training samples at each fidelity is decided by heuristics motivated by sparse grid combination techniques [19] resulting in the rigid relation $N_{f-1} = 2 \cdot N_f$. The main contribution of this work is an algorithm that adaptively samples the number of training samples needed for each fidelity on-the-fly. This procedure minimizes redundancy in training data generation, lowering the total computational footprint of MFML for QC.

Let a validation set at the highest fidelity be given as $\mathcal{V}^F := \{(x_i, y_i^F)\}_{i=1}^{N_{\text{val}}}$. In standard ML practices this dataset is used to optimize hyper-parameters of the ML model (e.g.: kernel, kernel width etc). In our adaptive-MFML framework, the training data set size at each fidelity, N^f , is treated as a dynamic variable optimized using the validation dataset. As illustrated by the workflow in Fig. 1, the optimization is carried out within a nested loop structure. For each local loop (or epoch), the algorithm sequentially injects a batch of training data starting at the lowest fidelity ($f = 1$). As presented in Algorithm 1, in each epoch, an MFML model is trained and evaluated for \mathcal{V}^F computing the empirical error. The improvement of the error (Δ) is tracked

for consecutive data injections. If Δ falls below a *local tolerance* threshold, the algorithm moves to the next fidelity and carries out the same procedure. This step-wise progression is performed until the highest fidelity is reached. At this stage, the algorithm checks for improvement in the empirical error for one global loop (that is cycling through all fidelities once). If this *global improvement* is below a *global tolerance*, the algorithm terminates returning ideal test set sizes and a trained MFML model. Otherwise, the algorithm continues to dynamically add training samples starting from the lowest fidelity passing through epochs and global loops. Notice that for each fidelity, during an epoch, the algorithm calls a QC calculator (see line 10 of Algorithm 1) on-the-fly. That is, the algorithm only requires the calculator to compute reference computations on a need-to-know basis. Notice that in line 8, we ensure that the algorithm breaks if the ratio of training dataset sizes for consecutive fidelities reach the standard MFML fixed scaling of 2.

4.3 Error Metrics

The prediction error of ML models studied in this work are computed as the mean absolute error (MAE) over a holdout test dataset $\mathcal{U}^F := \{(\mathbf{x}_i, y_i^F)\}_{i=1}^{N_{\text{test}}}$ which is given as

$$\text{MAE} := \sum_{i=1}^{N_{\text{test}}} |y_i^F - P_{\text{ML}}(\mathbf{x}_i)| . \quad (4)$$

The test set is not used at any stage of training or hyper-parameter optimization to truly reflect an out-of-sample error metric. In this study, the MAE of the trained models are studied as a function of the training data cost. For a single fidelity model the cost of a model is $T_{\text{train}}^{\text{SF}} := N_F \cdot c_F$ where c_F is the cost of a single data point at fidelity F . For the multifidelity models, the training data cost is the cumulative cost of training data used at each fidelity, that is, $T_{\text{train}}^{\text{MFML}} := \sum_{f=1}^F N_f \cdot c_f$. For the basic MFML model, due to the data scaling, this reduces to $T_{\text{train}}^{\text{MFML}} = \sum_{f=1}^F 2^{f-1} N_1 \cdot c_f$. As an example, consider the case for $N_{\text{train}} = [32, 16, 8, 4]$ for the ANI-1ccx dataset. The time-costs are reported in Table ST4 in the supplementary information. The cost of the MFML with this specific training data structure will be $32 \cdot 9.65 + 16 \cdot 16.82 + 8 \cdot 40.35 + 4 \cdot 157.27 = 1529.8$ seconds.

Since one is generally interested in the average behavior of the ML models, multiple runs of shuffling the training dataset before building the ML models are considered. For the single fidelity models, this is the basic cross-validation schemes on a fixed test set. However, for the MFML models since the nested training data structure is to be retained, the cross-validation scheme introduced in [20] is utilized to run different training dataset shuffling for the MFML models. The learning curve is then plotted as the average of the MAE resulting from these runs. For single fidelity KRR and basic MFML, the average of 10-run random shuffling of the dataset is used. For the adaptively sampled MFML models, since the random shuffling of the dataset results in a different optimization route for the training samples, a modified strategy outlined below is carried out:

1. For series of random seeds k generate adaptive-MFML model M_k .

2. Collect the pair $([N_1, N_2, \dots, N^F]_j^k, \text{MAE}_j^k) \rightarrow (T_{\text{train},j}^k, \text{MAE}_j^k)$ for each iteration j of the adaptive sampling scheme.
3. Build an interpolation model for T_{train} and MAE using the different random seed k .
4. Interpolate the average trend of the learning curves.

Data availability

All data used in this work comes from openly available datasets which are appropriately cited.

Code Availability

The programming scripts used for this work can be openly accessed at [this GitHub repository](#).

Supplementary information

Supplementary Sections S1–S9, Figures SF1–SF9, Tables ST1–ST4, Algorithm SA1.

Acknowledgments

The authors acknowledge support by the DFG through the project ZA 1175/3-1 as well as through the DFG Priority Program SPP 2363 on ‘Utilization and Development of Machine Learning for Molecular Applications – Molecular Machine Learning’ through the project ZA 1175/4-1. The authors would also like to acknowledge the support of the ‘Interdisciplinary Center for Machine Learning and Data Analytics (IZMD)’ at the University of Wuppertal. VV thanks Sergei Tretiak, Olexandr Isayev, and Justin Smith for guidance with the ANI-1ccx dataset. VV also thanks Louise Schaub for her design feedback.

Author Contribution

VV: writing, revision, conceptualization, methodology, validation, formal analysis, investigation, data curation, visualization

PZ: conceptualization, validation, supervision, funding acquisition

Declarations

The authors declare that there is no conflict of interest or any competing interests.

References

- [1] Kennedy, M., O’Hagan, A.: Predicting the output from a complex computer code when fast approximations are available. *Biometrika* **87**(1), 1–13 (2000) <https://doi.org/10.1093/biomet/87.1.1>

- [2] Gratiet, L.L., Garnier, J.: Recursive co-kriging model for design of computer experiments with multiple levels of fidelity. *Int. J. Uncertainty Quantif.* **4**(5) (2014) <https://doi.org/10.1615/Int.J.UncertaintyQuantification.2014006914>
- [3] Fernández-Godino, M.G.: Review of multi-fidelity models. *Adv. Comput. Sci. Eng.* **1**(4), 351–400 (2023) <https://doi.org/10.3934/acse.2023015>
- [4] Dral, P.O.: Quantum chemistry in the age of machine learning. *J. Phys. Chem. Lett.* **11**(6), 2336–2347 (2020) <https://doi.org/10.1021/acs.jpcclett.9b03664>
- [5] Westermayr, J., Gastegger, M., Schütt, K.T., Maurer, R.J.: Perspective on integrating machine learning into computational chemistry and materials science. *J. of Chem. Phys.* **154**(23), 230903 (2021) <https://doi.org/10.1063/5.0047760>
- [6] Crawford, T.D., Schaefer III, H.F.: An Introduction to Coupled Cluster Theory for Computational Chemists, pp. 33–136. John Wiley & Sons, Ltd, (2000). Chap. 2. <https://doi.org/10.1002/9780470125915.ch2>
- [7] Ramakrishnan, R., Dral, P.O., Rupp, M., Lilienfeld, O.A.: Big data meets quantum chemistry approximations: The Δ -machine learning approach. *J. Chem. Theory Comput.* **11**(5), 2087–2096 (2015) <https://doi.org/10.1021/acs.jctc.5b00099>
- [8] Pilania, G., Gubernatis, J.E., Lookman, T.: Multi-fidelity machine learning models for accurate bandgap predictions of solids. *Comput. Mater. Sci.* **129**, 156–163 (2017) <https://doi.org/10.1016/j.commatsci.2016.12.004>
- [9] Zaspel, P., Huang, B., Harbrecht, H., Von Lilienfeld, O.A.: Boosting quantum machine learning models with a multilevel combination technique: Pople Diagrams revisited. *J. Chem. Theory Comput.* **15**(3), 1546–1559 (2019) <https://doi.org/10.1021/acs.jctc.8b00832>
- [10] Vinod, V., Maity, S., Zaspel, P., Kleinekathöfer, U.: Multifidelity machine learning for molecular excitation energies. *J. Chem. Theory Comput.* **19**(21), 7658–7670 (2023) <https://doi.org/10.1021/acs.jctc.3c00882>
- [11] Ruth, M., Gerbig, D., Schreiner, P.R.: Machine learning for bridging the gap between density functional theory and coupled cluster energies. *J. Chem. Theory and Comp.* **19**(15), 4912–4920 (2023) <https://doi.org/10.1021/acs.jctc.3c00274>
- [12] Vinod, V., Lyu, D., Ruth, M., R. Schreiner, P., Kleinekathöfer, U., Zaspel, P.: Predicting molecular energies of small organic molecules with multi-fidelity methods. *J. Comp. Chem.* **46**(6), 70056 (2025) <https://doi.org/10.1002/jcc.70056>
- [13] Sandonas, L.M., Balcells, D., Bochkarev, A., Cole, J.M., Deringer, V.L., Dobrutz, W., Ehrenhofer, A., Frank, T., Friederich, P., Friedrich, R., George, J., Ghiringhelli, L., Caldas, A.H., Juraskova, V., Kneiding, H., Lysogorskiy, Y., Margraf, J.T., Türk, H., Lilienfeld, A., Todorović, M., Tkatchenko, A., Rossi, M.,

- Cuniberti, G.: Perspective: Towards sustainable exploration of chemical spaces with machine learning (2026). <https://arxiv.org/abs/2604.00069>
- [14] Dral, P.O., Owens, A., Dral, A., Csányi, G.: Hierarchical machine learning of potential energy surfaces. *J. Chem. Phys.* **152**(20), 204110 (2020) <https://doi.org/10.1063/5.0006498>
- [15] Vinod, V., Zaspel, P.: Benchmarking data efficiency in Δ -ML and multifidelity models for quantum chemistry. *J. Chem. Phys.* **163**(2), 024134 (2025) <https://doi.org/10.1063/5.0272457>
- [16] Vinod, V., Zaspel, P.: Investigating data hierarchies in multifidelity machine learning for excitation energies. *J. Chem. Theory Comput.* **21**(6), 3077–3091 (2025) <https://doi.org/10.1021/acs.jctc.4c01491>
- [17] Lyu, D., Vinod, V., Holzenkamp, M., Holtkamp, Y.M., Maity, S., Salazar, C.R., Kleinekathöfer, U., Zaspel, P.: Excitation energy transfer between porphyrin dyes on a clay surface: A study employing multifidelity machine learning. *Adv. Theory Simul.* **8**(11), 00271 (2025) <https://doi.org/10.1002/adts.202500271>
- [18] Maity, S., Vinod, V., Zaspel, P., Kleinekathöfer, U.: Δ -machine learning for LC-DFT-level excitation energies of bacteriochlorophyll molecules in a LH2 complex. *ChemRxiv* **2026**(0504) (2026) <https://doi.org/10.26434/chemrxiv.15002714/v1>
- [19] Bungartz, H.-J., Griebel, M.: Sparse grids. *Acta Numerica* **13**, 147–269 (2004) <https://doi.org/10.1017/S0962492904000182>
- [20] Vinod, V., Kleinekathöfer, U., Zaspel, P.: Optimized multifidelity machine learning for quantum chemistry. *Mach. Learn.: Sci. Technol.* **5**(1), 015054 (2024) <https://doi.org/10.1088/2632-2153/ad2cef>
- [21] Zhang, L., Zhang, S., Owens, A., Yurchenko, S.N., Dral, P.O.: VIB5 database with accurate ab initio quantum chemical molecular potential energy surfaces. *Sci. Data* **9**(1), 84 (2022) <https://doi.org/10.1038/s41597-022-01185-w>
- [22] Vinod, V., Zaspel, P.: QeMFi: A multifidelity dataset of quantum chemical properties of diverse molecules. *Sci. Data* **12**(1), 202 (2025) <https://doi.org/10.1038/s41597-024-04247-3>
- [23] Vinod, V., Zaspel, P.: QeMFi: A multifidelity dataset of quantum chemical properties of diverse molecules (1.1.0) [dataset]. *Zenodo* (2024) <https://doi.org/10.5281/zenodo.13925688>
- [24] Pinheiro Jr, M., Zhang, S., Dral, P.O., Barbatti, M.: WS22 database, Wigner Sampling and geometry interpolation for configurationally diverse molecular datasets. *Sci. Data* **10**(1), 95 (2023) <https://doi.org/10.1038/s41597-023-01998-3>

- [25] Westermayr, J., Marquetand, P.: Machine learning for electronically excited states of molecules. *Chem. Rev.* **121**(16), 9873–9926 (2020) <https://doi.org/10.1021/acs.chemrev.0c00749>
- [26] Dral, P.O., Barbatti, M.: Molecular excited states through a machine learning lens. *Nat. Rev. Chem.* **5**(6), 388–405 (2021) <https://doi.org/10.1038/s41570-021-00278-1>
- [27] Smith, J.S., Zubatyuk, R., Nebgen, B., Lubbers, N., Barros, K., Roitberg, A.E., Isayev, O., Tretiak, S.: The ANI-1ccx and ANI-1x data sets, coupled-cluster and density functional theory properties for molecules. *Sci. Data* **7**(1), 134 (2020) <https://doi.org/10.1038/s41597-020-0473-z>
- [28] Bartlett, R.J., Musiał, M.: Coupled-cluster theory in quantum chemistry. *Rev. Mod. Phys.* **79**, 291–352 (2007) <https://doi.org/10.1103/RevModPhys.79.291>
- [29] Gao, X., Ramezanghorbani, F., Isayev, O., Smith, J.S., Roitberg, A.E.: TorchANI: A free and open source PyTorch-based deep learning implementation of the ani neural network potentials. *J. Chem. Inf. Modeling* **60**(7), 3408–3415 (2020) <https://doi.org/10.1021/acs.jcim.0c00451>
- [30] Vinod, V., Zaspel, P.: LFAB: low fidelity as bias for active learning in the chemical configuration space. *J. Chem. Theory Comput.* (2026) <https://doi.org/10.1021/acs.jctc.6c00009>
- [31] Smith, J.S., Nebgen, B., Lubbers, N., Isayev, O., Roitberg, A.E.: Less is more: Sampling chemical space with active learning. *J. Chem. Phys.* **148**(24), 241733 (2018) <https://doi.org/10.1063/1.5023802>
- [32] Qu, C., Houston, P.L., Conte, R., Nandi, A., Bowman, J.M.: Breaking the coupled cluster barrier for machine-learned potentials of large molecules: The case of 15-atom acetylacetone. *J. Phys. Chem. Lett.* **12**(20), 4902–4909 (2021) <https://doi.org/10.1021/acs.jpcllett.1c01142>
- [33] Vinod, V., Zaspel, P.: Assessing non-nested configurations of multifidelity machine learning for quantum-chemical properties. *Mach. Learn.: Sci. Technol.* **5**(4), 045005 (2024) <https://doi.org/10.1088/2632-2153/ad7f25>